*Chemical Engineering Science*, Vol. 48, No. 5, pp. 845–861, 1993.
Printed in Great Britain.

0009–2509/93 $6.00 + 0.00


# PROBLEMS AND PITFALLS IN THE USE OF THE FICK FORMULATION FOR INTRAPARTICLE DIFFUSION

R. KRISHNA
Department of Chemical Engineering, University of Amsterdam, Nieuwe Achtergracht 166, 1018 WV Amsterdam, The Netherlands

(*First received* 4 *March* 1992; *accepted for publication in revised form* 22 *April* 1992)

**Abstract**—In this paper attention is focused on intraparticle diffusion of multicomponent gaseous mixtures in macroporous and microporous media. Bulk, Knudsen and surface diffusion will be handled using a unified, consistent, approach, borrowing ideas and concepts developed more than a century ago by James Clerk Maxwell and Josef Stefan. The diffusion equations for bulk and Knudsen equations coincide with the dusty gas model, rediscovered already about five times in history. The walls of the porous adsorbent are modelled as giant dust molecules and in this theory they are accorded the status of pseudo-species. One advantage of this procedure is that the kinetic gas theory may now be used to predict the Knudsen diffusion coefficients. For the description of surface diffusion of multicomponent mixtures a new approach is developed in which the vacant sites are modelled, additionally, as pseudo-species (craters on the dust "molecules"). The practical application of the crated dusty gas model is illustrated by considering a number of studies, including (1) single-component sorption; (2) uptake of binary mixtures by zeolites and activated carbon; (3) multicomponent diffusion and chemical reaction within catalyst pellets. The examples discussed in this paper support the contention that the Fick formulation is hopelessly inadequate because it will fail even at the *qualitative level* to describe the observed experimental phenomena. The Maxwell–Stefan formulation provides a useful tool for solving practical problems in intraparticle diffusion.

## INTERPARTICLE AND INTRAPARTICLE DIFFUSION

Most commercial adsorbents consist of small microporous crystals (e.g. zeolites) formed into a macroporous pellet (Ruthven, 1984). The molecular species constituting the fluid mixture have first to be transported from the bulk fluid phase to the external surface of the adsorbent. Within the particle there are two distinct diffusional resistances to mass transfer: the macropore (intercrystalline) diffusional resistance of the pellet and the micropore (intracrystalline) diffusion resistance. A schematic picture of a catalyst or adsorbent particle is shown in Fig. 1. In the discussion to follow in this paper the focus is on *intra*particle diffusion phenomena. The relative importance of macropore and micropore diffusion resistances depends *inter alia* on the pore size distribution within the catalyst or adsorbent particle. Figure 2 shows typical pore size distributions for three commonly adsorbent particles. *Micro*pores have diameters smaller than 2 nm; *macro*pores have sizes greater than 50 nm and *meso*pores are in the size range 2–50 nm.

## DIFFUSION MECHANISMS

Within a pore we may, in general, distinguish three fundamentally different types of diffusion mechanism, as depicted pictorially in Fig. 3:

- Bulk, "free space" or free molecular diffusion that becomes significant for large pore sizes and high system pressures; here molecule–molecule collisions dominate over molecule–wall collisions.
- Knudsen diffusion that becomes predominant when the mean free path of the molecular species is much larger than the pore diameter and, hence, molecule–wall collisions become important.
- Surface diffusion of adsorbed molecular species along the pore wall surface; this mechanism of transport becomes dominant for micropores and for strongly adsorbed species.

Bulk and Knudsen diffusion mechanisms occur in series and it is always prudent to take both mechanisms into account rather than assume that one or other mechanism is "controlling". Surface diffusion occurs in parallel to the other two mechanisms and its contribution to the total species flux may be quite significant in many cases, as we shall see later in this paper. Within the micropores the dominant mechanism is surface diffusion. It is for this reason that surface diffusion is also referred to as micropore diffusion in the literature (e.g. Ruthven, 1984).

## FICK FORMULATION FOR INTRAPARTICLE DIFFUSION

In the design of an adsorber or catalytic reactor an essential step is the calculation of the fluxes inside the pellet depicted in Fig. 1. For any diffusing species $i$ the equations of continuity take the form (cf. Bird *et al.*, 1960)

$$\frac{\partial c_i}{\partial t} + \nabla \cdot \mathbf{N}_i = \mathscr{R}_i \tag{1}$$

where $c_i$ is the molar concentration of species $i$, $\mathbf{N}_i$ molar flux of species $i$ in a stationary coordinate frame of reference, and $\mathscr{R}_i$ is the rate of production of $i$ due to chemical reaction within the pellet. The molar

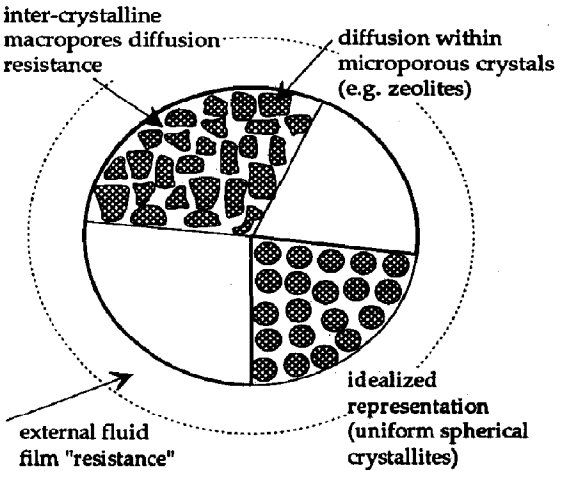


Fig. 1. Schematic diagram of adsorbent or catalyst particle depicting the three main diffusion resistances (after Ruthven, 1984).

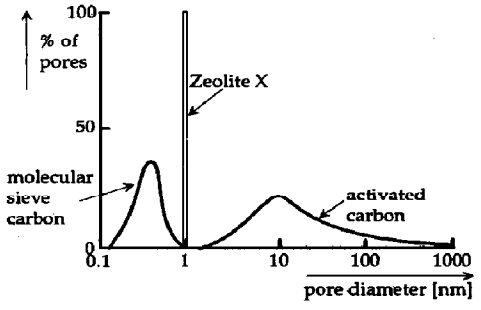


Fig. 2. Pore size distribution of zeolite X, molecular sieve carbon and activated carbon (after Yang, 1987).

fluxes, $\mathbf{N}_i$, are

$$\mathbf{N}_i = c_i \mathbf{v}_i = c x_i \mathbf{v}_i, \quad \sum_{i=1}^{n} \mathbf{N}_i = \mathbf{N}_t \tag{2}$$

where $\mathbf{v}_i$ is the velocity of the transferring species $i$ inside the pellet, $c$ is the total mixture molar concentration, $\mathbf{x}_i$ is the mole fraction of species $i$, and $n$ is the number of diffusing species. We may define the molar average mixture velocity as follows:

$$\mathbf{v} = \sum_{i=1}^{n} x_i \mathbf{v}_i. \tag{3}$$

The diffusion flux of species $i$ relative to this molar average reference velocity, $\mathbf{v}$, is

$$\mathbf{J}_i \equiv c_i(\mathbf{v}_i - \mathbf{v}) \equiv \mathbf{N}_i - x_i \mathbf{N}_t. \tag{4}$$

The simplest constitutive relation for the diffusion flux, $\mathbf{J}_i$, is that due to Fick:

$$\mathbf{J}_i = -cD\nabla x_i \tag{5}$$

where $D$ is the Fick diffusivity and $\nabla x_i$ the gradient of the component mole fraction can be regarded as the driving force for diffusion. The Fick diffusivity $D$ is, in general, composition-dependent and, within the confines of the original Fick development, this coefficient is positive definite. Intraparticle diffusion processes within adsorbent and catalyst particles are usually interpreted in terms of the Fick formulation represented by eq. (5) for each of the three diffusion mechanisms represented in Fig. 3.

Within the framework of the Fick formulation, it is always to be expected that the diffusion flux of any species $i$, $\mathbf{J}_i$, will be down the composition gradient. In other words, the sign of $\mathbf{J}_i$ will be the same as that of $-\nabla x_i$. It is one of the objectives of this paper to show that the Fick formulation will fail, *even at the qualitative level*, to describe the observed diffusion behaviour for each of the three diffusion mechanisms: bulk, Knudsen and surface. We begin by demonstrating the inadequacy of the Fick formulation for bulk diffusion in ideal gas mixtures.

## LIMITATIONS OF THE FICK FORMULATION FOR BULK DIFFUSION

Let us consider a simple and illuminating set of experiments conducted by Duncan and Toor (1962). These authors examined diffusion in an ideal ternary gas mixture: hydrogen (1)–nitrogen (2)–carbon dioxide (3). The experimental set-up consisted of a two-bulb diffusion cell, pictured in Fig. 4(a). In an experiment that we shall highlight here the two bulbs, bulb 1 and bulb 2, had the initial compositions (expressed in mole fractions) as given below:

Bulb 1:

$$x_1 = 0.50121, \quad x_2 = 0.49879, \quad x_3 = 0.00000$$

Bulb 2:

$$x_1 = 0.00000, \quad x_2 = 0.50086, \quad x_3 = 0.49914.$$

The two bulbs were connected by means of a long capillary of 2.08 mm diameter. At time $t = 0$, the stopcock separating the two composition environments at the centre of the capillary was opened and diffusion of the three species was allowed to take place. From the information given in the paper by Duncan and Toor (1962) it is verifiable that the diffusion mechanism prevalent in the capillary is bulk diffusion. Further, the pressure differences between the two bulbs were negligibly small implying no occurrence of viscous flow. Since the two bulbs are sealed there was no net transfer flux out of or into the system, i.e. we have conditions corresponding to equimolar diffusion:

$$\mathbf{v} = \mathbf{0}, \quad \mathbf{N}_1 + \mathbf{N}_2 + \mathbf{N}_3 = \mathbf{0}. \tag{6}$$

The composition–time trajectories for each of the three diffusing species in either bulb has been presented in Fig. 4(b). Let us first examine what happens to hydrogen (1) and carbon dioxide (3). The composition–time trajectories are as we should expect; hydrogen diffuses from bulb 1 to bulb 2 and the two compositions approach each other, albeit slowly. Carbon

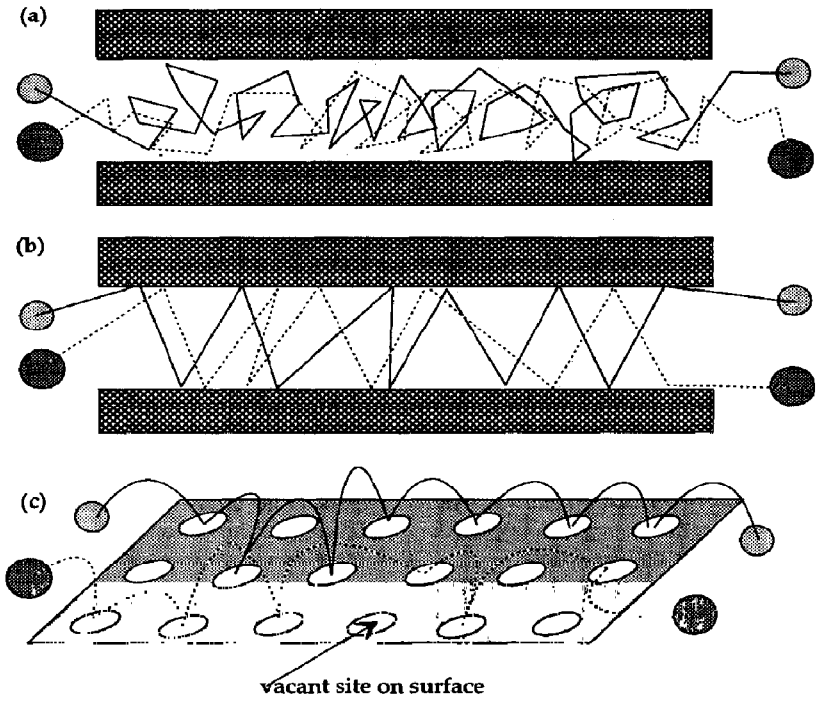


Fig. 3. Three distinct mechanisms by which molecular species get transported within an adsorbent or catalyst particle: (a) bulk diffusion; (b) Knudsen diffusion and (c) surface diffusion of adsorbed species along the surface of the pores.

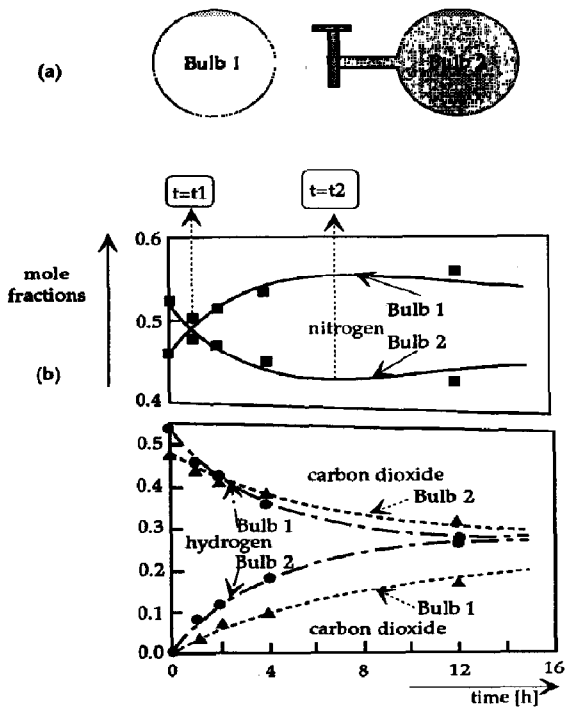


Fig. 4. Two-bulb diffusion cell experiment of Duncan and Toor (1962): (a) the experimental set-up; (b) composition–time trajectories for the species hydrogen (1)–nitrogen (2)–carbon dioxide (3).

dioxide diffuses from bulb 2 to bulb 1 in the expected normal fashion. The diffusion behaviour of these two species, hydrogen and carbon dioxide, may be termed to be Fickian, i.e. down their respective composition gradients: nothing extraordinary here.

If we examine the composition–time trajectory of nitrogen (2), we see several curious phenomena occurring. Initially, at time $t = 0$, the composition of nitrogen in bulb 2 is higher than in bulb 1 and we should expect, following our Fickian ideas, that diffusion should take place from bulb 2 to bulb 1, decreasing the composition in bulb 2 and consequently increasing the composition of nitrogen in bulb 1. This expectation is indeed fulfilled during the time interval from $t = 0$ to $t = t1 \cong 1$ h; see Fig. 4(b). At $t = t1 \cong 1$ h the composition of nitrogen in the two bulbs is identical and, therefore, at this point the composition gradient driving force for nitrogen must be zero. At $t = t1$, it was observed experimentally by Duncan and Toor (1962) that the diffusion of nitrogen did not cease but, contrary to the Fickian expectations, continued further implying that

$$\nabla x_2 = \mathbf{0}, \quad \mathbf{J}_2 \neq \mathbf{0}, \quad t = t1. \tag{7}$$

The bulb 1 composition continued to increase at the expense of bulb 2 composition of nitrogen beyond the point $t = t1$ and this diffusion of nitrogen is in an uphill direction, i.e.

$$\frac{\mathbf{J}_2}{-\nabla x_2} > \mathbf{0}, \quad t1 < t < t2. \tag{8}$$

Uphill diffusion of nitrogen continued to take place till the time $t = t2$ is reached when the composition profiles in either bulb tend to reach a plateau. This plateau implies that the diffusion flux of nitrogen is zero at this point despite the fact that there is a large driving force existing. At $t = t2$ we have

$$\nabla x_2 \neq 0, \quad J_2 = 0, \quad t = t2. \tag{9}$$

Beyond the point $t = t2$, the diffusion behaviour of nitrogen is "normal", i.e. the composition of nitrogen in bulb 1 with a higher concentration decreases while the composition of nitrogen in bulb 2 with the lower concentration increases.

Toor (1957) in a classic paper anticipated the three curious phenomena described above and assigned the following names to them:

- *Osmotic diffusion*: This is the phenomenon observed at $t = t1$ and described by eq. (7). Here diffusion of a component takes place despite the absence of a constituent driving force.
- *Reverse diffusion*: This phenomenon is observed for nitrogen in the time interval $t1 < t < t2$ and described by eq. (8). Here diffusion of a component takes place in a direction opposite to that dictated by its driving force.
- *Diffusion barrier*: This phenomenon is observed at $t = t2$ and is described by eq. (9). Here a component diffusion flux is zero despite the existence of a large driving force.

It should be clear that the use of the Fick formulation, eq. (5), will be totally inadequate to describe the three curious phenomena described above because in order to rationalise the experimental observations we must demand the following behaviour of the Fick diffusivity for nitrogen:

- $D \to \infty$ at the osmotic diffusion point, cf. eq. (7),
- $D < 0$ in the region where reverse diffusion occurs, cf. eq. (8), and
- $D = 0$ at the diffusion barrier, cf. eq. (9)

It must not be forgotten that this strange behaviour of the Fick diffusivity for nitrogen has been observed experimentally for an *ideal gas mixture* at constant temperature and pressure conditions and for a situation corresponding to *equimolar diffusion*. It is clearly necessary to abandon the Fickian mode of thinking and to adopt a more fundamental and mechanistic approach to diffusion. The most useful and practical approach to bulk diffusion was developed independently more than a century ago by Maxwell (1866) and Stefan (1871). We develop this approach first for bulk diffusion of fluid mixtures.

## THE MAXWELL–STEFAN APPROACH TO BULK DIFFUSION OF MULTICOMPONENT MIXTURES

Before proceeding to the general multicomponent case, let us start with a simple two component system, made up of species denoted by 1 and 2. To effect relative motion between the molecular species 1 and 2 in the mixture, we must exert a force on each of the two species. To calculate this force that is exerted on any molecular species $i$, let us consider $z$-directional diffusion in the system and write down the force balances for the control volume shown in Fig. 5. The cross-sectional area available for diffusion is 1 m$^2$ and the length of the diffusion path is dz. If the change in the partial pressure of component $i$ across the diffusion distance dz is $dp_i$, the force acting per m$^3$ is $dp_i/dz$. The concentration of species $i$ in the mixture is $c_i$ and, therefore, the force acting per mole of species $i$ is $(1/c_i)(dp_i/dz)$. For an ideal gas mixture we have $c_i = p_i/RT$ and, therefore, the force per mole of species $i$ can be written as $(RT/p_i)(dp_i/dz) = RT\,d \ln p_i/dz$ or, expressed in terms of the chemical potential of species $i$, this force is $d\mu_i/dz$. This force is balanced by friction between the diffusing species 1 and 2 in the binary mixture; see the pictorial representation in Fig. 6. The force balance on the species 1 takes the form

$$-\frac{d\mu_1}{dz} = RTx_2\frac{(v_1 - v_2)}{\mathcal{D}_{12}}. \tag{10}$$

For transport of species 1 in the positive $z$-direction, i.e. positive velocity $v_1$, we must have a positive value for $-d\mu_1/dz$ and, therefore, the left member of eq. (10) must be viewed as the driving force for transport in the positive $z$-direction. This force is balanced by the friction experienced between the species 1 and

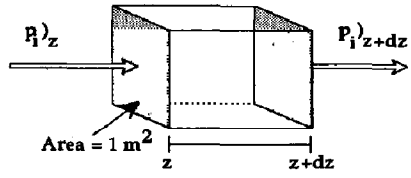


Fig. 5. A simple force balance on a control volume containing an ideal gas mixture.

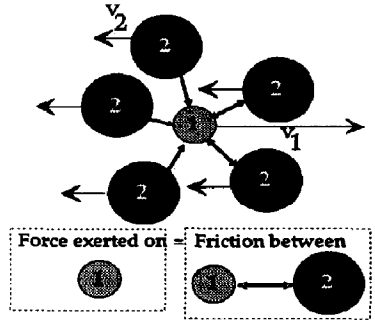


Fig. 6. The basis of the development of the Maxwell–Stefan diffusion equations is the simple mechanical picture here. The force exerted on species 1 is balanced by the friction between species 1 and 2.

2. We may expect the frictional drag to be proportional to the velocity difference $(v_1 - v_2)$ and to the concentration of the mixture, expressed in eq. (10) as the mole fraction of component 2, $x_2$. The term $RT/Đ_{12}$ on the right-hand side of eq. (10) may be interpreted to be the drag coefficient. With this definition, the Maxwell–Stefan diffusivity $Đ_{12}$ has the units ($m^2 s^{-1}$) and the physical significance of an inverse drag coefficient.

Multiplying both sides of eq. (10) by $x_1/RT$

$$-\frac{x_1}{RT}\frac{d\mu_1}{dz} = \frac{x_1 x_2 v_1 - x_1 x_2 v_2}{Đ_{12}}. \qquad (11)$$

Re-arranging eq. (11) using the definition for the fluxes $N_i = cx_i v_i$ [cf. eq. (2)] we obtain, after vector generalisation,

$$-\frac{x_1}{RT}\nabla\mu_1 = \frac{x_2 \mathbf{N}_1 - x_1 \mathbf{N}_2}{cĐ_{12}}. \qquad (12)$$

For a non-ideal fluid mixture we may introduce the component activity coefficients to express the left member of eq. (12) as

$$\frac{x_1}{RT}\nabla\mu_1 = \left(1 + x_1\frac{\partial \ln \gamma_1}{\partial x_1}\right)\nabla x_1 = \Gamma \nabla x_1 \qquad (13)$$

where $\Gamma$ is the thermodynamic correction factor portraying the non-ideal behaviour. For highly non-ideal mixtures the thermodynamic factor $\Gamma$ is usually a strong function of the mixture composition and vanishes in the region of the critical point (Krishna, 1987). This behaviour has been illustrated in Fig. 7 for the system methanol (1)–*n*-hexane (2). For the temperature under consideration the system tends to undergo phase splitting at $x_1 \approx 0.5$; at this mole fraction we note that $\Gamma$ tends towards zero. Combining eqs (12) and (13), after introducing $x_2 = 1 - x_1$, we obtain, using eq. (4),

$$\mathbf{J}_1 \equiv \mathbf{N}_1 - x_1 \mathbf{N}_t = -cĐ_{12}\Gamma\nabla x_1. \qquad (14)$$

Comparison of eq. (14) with Fick's law [eq. (5)] yields the following relationship between the Fick diffusivity $D_{12}$ and the Maxwell–Stefan diffusivity, $Đ_{12}$:

$$D_{12} = Đ_{12}\Gamma. \qquad (15)$$

Because of the strong composition dependence of the thermodynamic factor $\Gamma$ we should expect the Fick diffusivity to also exhibit a strong, corresponding, composition dependence; this is indeed borne out by experimental evidence available in the literature and is illustrated in Fig. 8 for the system methanol (1)–*n*-hexane, for which we note that the Fick diffusivity tends to approach zero in the region of the phase transition point near $x \approx 0.5$. The Maxwell–Stefan diffusivity, $Đ_{12}$, calculated from the Fick diffusivity and the thermodynamic data, shows only a mild composition dependence. An empirical formula for the composition dependence is due to Vignes (1966) [see also Wesselingh and Krishna (1990)]:

$$Đ_{12} = [Đ_{12(x_1\to 1)}]^{x_1}[Đ_{12(x_1\to 0)}]^{1-x_1} \qquad (16)$$

where the bracketed terms are, respectively, the infinitely dilution values of the Maxwell–Stefan diffusivity at either ends of the composition range. The Vignes relation (16) implies that the logarithm of $Đ_{12}$ should be linear in the mole fraction $x_1$. From the data in Fig. 8 we see that this empirical model of Vignes holds remarkably well, considering the large variation of the Fick diffusivity. For further information regarding the prediction of the Maxwell–Stefan diffusivity for gaseous and liquid mixtures the reader is referred to the introductory book by Wesselingh and Krishna (1990).

For gaseous mixtures at low to moderate pressures and for thermodynamically ideal liquid mixtures, the thermodynamic factor $\Gamma = 1$ and the Maxwell–Stefan diffusivity is independent of composition; for this limiting case the Fick and Maxwell–Stefan diffusivity are identical to each other. The Maxwell–Stefan diffusivity has a fundamental physical meaning of an inverse drag coefficient and is more easily interpretable and predictable than the Fick diffusivity; the latter parameter is a conglomerate of two separate concepts: drag effects and thermodynamic non-ideality effects.

The mechanistic picture developed above for diffusion in a two component system can be extended to the general multicomponent cases quite easily. The force exerted on species 1 is balanced by the friction between species 1 and each of the other species in the mixture. For a ternary mixture, the simplest multi-

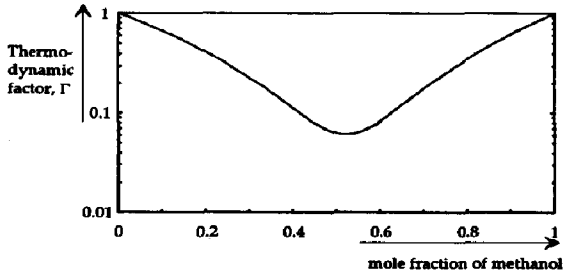


Fig. 7. The thermodynamic factor $\Gamma$ decreases sharply as the critical point is approached. This strong variation of $\Gamma$ largely explains the behaviour of the Fick diffusivity $D$ (seen in Fig. 8).

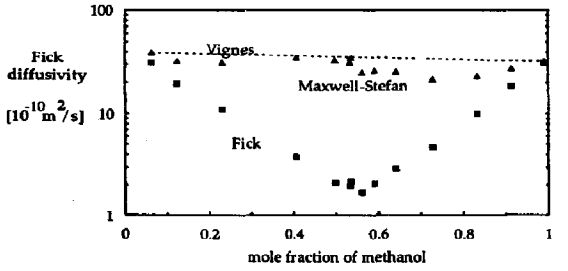


Fig. 8. The Fick diffusivity for the system methanol–*n*-hexane. Data from Clark and Rowley (1986). The Fick $D$ decreases sharply as the critical point is reached.

component system, for example, the Maxwell–Stefan diffusion equations are pictured in Fig. 9.

The generalisation of eq. (10) to the general multicomponent case is, therefore,

$$-\frac{d\mu_1}{dz} = RTx_2\frac{(v_1 - v_2)}{\mathcal{D}_{12}} + RTx_3\frac{(v_1 - v_3)}{\mathcal{D}_{13}} + RTx_4\frac{(v_1 - v_4)}{\mathcal{D}_{14}} + \cdots. \quad (17)$$

The terms on the right-hand side of eq. (17) represent, respectively, the friction between 1–2, 1–3, 1–4 and so on. Equation (17) can be written in terms of the fluxes $\mathbf{N}_i$ to obtain the following equation analogous to eq. (12) for the binary case

$$-\frac{x_i}{RT}\nabla\mu_i = \sum_{\substack{j=1\\ j\neq i}}^{n}\frac{x_j\mathbf{N}_i - x_i\mathbf{N}_j}{c\mathcal{D}_{ij}}, \quad i = 1, 2, \ldots, n. \quad (18)$$

Only $n - 1$ of eq. (18) are independent because of the Gibbs–Duhem restriction

$$\sum_{i=1}^{n} x_i\nabla\mu_i = 0. \quad (19)$$

It is helpful to express the left member of eq. (18) in terms of the mole fraction gradients by introducing an $(n-1)\times(n-1)$ matrix of thermodynamic factors $[\Gamma]$:

$$\frac{x_i}{RT}\nabla\mu_i = \sum_{j=1}^{n-1}\Gamma_{ij}\nabla x_j, \quad \Gamma_{ij} = \delta_{ij} + x_i\frac{\partial \ln\gamma_i}{\partial x_j} \quad i, j = 1, 2, \ldots, n-1. \quad (20)$$

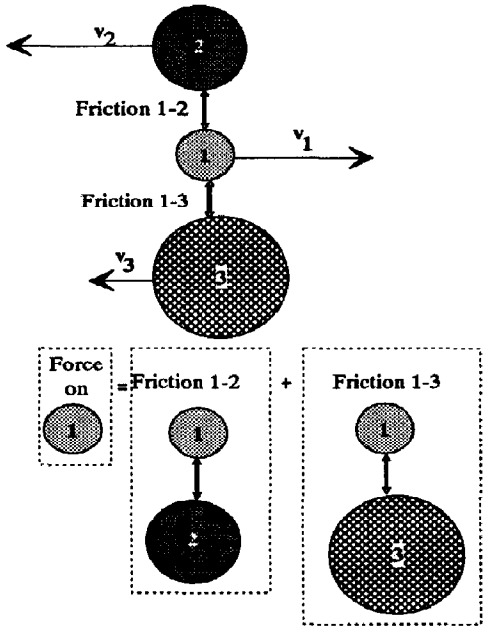


Fig. 9. The development of the Maxwell–Stefan diffusion equations for a ternary mixture. The force exerted on molecular species 1 is balanced by the friction between species 1 and 2 and between species 1 and 3.

Combining eqs (18)–(20) we obtain, in a manner analogous to eq. (13),

$$-c[\Gamma](\nabla x) = [B](\mathbf{J}) \text{ or } (\mathbf{J}) = -c[B]^{-1}[\Gamma](\nabla x) \quad (21)$$

where we use $(n-1)$-dimensional matrix notation; $(\mathbf{J})$ represents the column vector of $(n-1)$ diffusion fluxes defined by eq. (4). The elements of the matrix $[B]$ can be derived from eq. (18) in terms of the Maxwell–Stefan diffusivities $\mathcal{D}_{ij}$ as follows:

$$B_{ii} = \frac{x_i}{\mathcal{D}_{in}} + \sum_{\substack{k=1\\ k\neq i}}^{n}\frac{x_k}{\mathcal{D}_{ik}}, \quad B_{ij(i\neq j)} = x_i\left(\frac{1}{\mathcal{D}_{in}} - \frac{1}{\mathcal{D}_{ij}}\right). \quad (22)$$

The above derivations for multicomponent mixtures may seem to be quite formal and dry. In order to get a better feel for the parameters and numbers involved, let us take two typical systems.

Firstly, let us consider bulk diffusion at 25°C in a non-ideal liquid mixture made up of the components acetone (1)–benzene (2)–carbon tetrachloride (3). At the composition of $x_1 = 0.35$, $x_2 = 0.35$ and $x_3 = 0.30$ the Maxwell–Stefan diffusivities $\mathcal{D}_{ij}$ are estimated to be

$$\mathcal{D}_{12} = 3.4\times10^{-9}, \quad \mathcal{D}_{13} = 2.5\times10^{-9}$$
$$\mathcal{D}_{23} = 1.7\times10^{-9}.$$

The matrix $[B]$ can be calculated from the pair Maxwell–Stefan diffusivities using eq. (22):

$$[B] = \begin{bmatrix} 0.363 & -0.036 \\ 0.107 & 0.495 \end{bmatrix}\times10^{9}.$$

The matrix of thermodynamic factors is estimated from activity coefficient data to be

$$[\Gamma] = \begin{bmatrix} 0.69 & -0.13 \\ 0.07 & 1.05 \end{bmatrix}.$$

The two independent diffusion fluxes for components 1 and 2 can now be expressed explicitly in terms of the composition gradient driving forces using eq. (21) as

$$\begin{pmatrix}\mathbf{J}_1\\ \mathbf{J}_2\end{pmatrix} = -c\begin{bmatrix} 0.363 & 0.036 \\ 0.107 & 0.495 \end{bmatrix}^{-1}\times10^{-9} \times\begin{bmatrix} 0.69 & -0.13 \\ 0.07 & 1.05 \end{bmatrix}\times\begin{pmatrix}\nabla x_1\\ \nabla x_2\end{pmatrix} = -c\begin{bmatrix} 1.92 & -0.58 \\ -0.28 & 2.25 \end{bmatrix}\times10^{-9}\times\begin{pmatrix}\nabla x_1\\ \nabla x_2\end{pmatrix}$$

which shows that there is a strong influence of the driving force of component 2 on the flux of component 1. This *coupling* is caused by two effects: (i) the thermodynamic non-idealities in the system (note that $[\Gamma]$ is significantly non-diagonal) and (ii) the differences in the Maxwell–Stefan diffusivities (this implies that the frictional drag of the pairs 1–2, 1–3 and 2–3 are all significantly different from one another).

It is common to define a matrix of Fick diffusivities $[D]$ analogous to the binary case [cf. eqs (14) and

(15)] by using $(n-1)\times(n-1)$ matrix notation:

$$[D] = [B]^{-1}[\Gamma]. \tag{23}$$

For the system acetone (1)–benzene (2)–carbon tetrachloride (3) the elements of the matrix for the specified composition have the values

$$[D] = \begin{bmatrix} 1.92 & -0.58 \\ -0.28 & 2.25 \end{bmatrix} \times 10^{-9}$$

For the general multicomponent mixture it is difficult to ascribe simple physical interpretations to the elements of $[D]$; it is for this reason we prefer the Maxwell–Stefan formulation that also aids in the prediction of the elments of $[D]$. Specifically, the advantage of the M–S formulation is that we decouple the drag effects (portrayed by $[B]$) from thermodynamic effects (portrayed by $[\Gamma]$).

Let us now consider the case of an ideal gas mixture for which the matrix of thermodynamic factors $[\Gamma]$ reduces to the identity matrix $[I]$; eq. (18) reduces to

$$-\frac{1}{RT}\nabla p_i = \sum_{\substack{j=1 \\ j\neq i}}^{n} \frac{x_j \mathbf{N}_i - x_i \mathbf{N}_j}{\mathcal{D}_{ij}}, \quad i = 1, 2, \ldots, n. \tag{18a}$$

We shall explain the curious diffusion phenomena observed by Duncan and Toor (1962) for the system hydrogen (1)–nitrogen (2)–carbon dioxide (3) as seen in Figs 4(a)–(c). For this ternary mixture the Maxwell–Stefan diffusivities of the three binary pairs can be estimated from the kinetic gas theory to be

$$\mathcal{D}_{12} = 8.33\times10^{-5}, \quad \mathcal{D}_{13} = 6.8\times10^{-5}$$
$$\mathcal{D}_{23} = 1.68\times10^{-5}.$$

At the equilibrium composition the elements of the matrix $[B]$ are estimated to be

$$[B] = \begin{bmatrix} 0.134 & 0.007 \\ 0.237 & 0.476 \end{bmatrix} \times 10^{5}$$

and the matrix of Fick diffusivities is, therefore,

$$[D] = \begin{bmatrix} 7.68 & -0.11 \\ -3.832 & 2.15 \end{bmatrix} \times 10^{-5}.$$

If we write down explicitly the flux relation for nitrogen, component 2, we see that $\mathbf{J}_2 = -cD_{21}\nabla x_1 - cD_{22}\nabla x_2 = -c(-3.83\times\nabla x_1 + 2.15\times\nabla x_2)\times10^{-5}$. This implies that the flux of nitrogen is strongly coupled to the driving force of the component 1. When the driving force of nitrogen $\nabla x_2 = 0$, we see that the flux of nitrogen remains non-zero and equals $\mathbf{J}_2 = -cD_{21}\nabla x_1 = -c(3.83\times\nabla x_1)\times10^{-5}$. This non-zero flux causes the diffusion of nitrogen beyond the point $t = t1$ (the osmotic diffusion point) in Fig. 4(b). Between $t = t1$ and $t = t2$ we have $|3.83\times\nabla x_1| > |2.15\times\nabla x_2|$ and, therefore, the direction of nitrogen is against its intrinsic gradient (reverse or uphill diffusion). At the point $t = t2$, we have $|3.83\times\nabla x_1| = |2.15\times\nabla x_2|$ and, since these two terms have opposite signs, $\mathbf{J}_2 = -(-c3.83\times\nabla x_1 + 2.15\times\nabla x_2)\times10^{-5} = 0$ and nitrogen experiences a diffusion barrier.

What we did above was to transform the Maxwell–Stefan diffusion equations into a matrix generalisation of Fick's law to explain the curious effects observed by Duncan and Toor (1962). The path via matrix algebra lacks the physical insight provided by the Maxwell–Stefan formulation, on the basis of which it is possible to explain the behaviour of nitrogen in Fig. 4(b) simply by using force–friction arguments. The driving force of nitrogen is much smaller compared to that of hydrogen and carbon dioxide. The frictional drag exerted by carbon dioxide (3) on nitrogen (2) transport is considerably larger than the frictional drag exerted by hydrogen (1) on nitrogen (2) transport; this can be seen from the fact that $(1/\mathcal{D}_{23}) \gg (1/\mathcal{D}_{12})$. During the time interval $t = t1$ and $t = t2$, the direction in which the driving force of carbon dioxide acts is opposite to that in which the driving force of nitrogen acts. The much larger flux of carbon dioxide drags nitrogen against its intrinsic gradient, uphill. From this reasoning it should be clear that if the components hydrogen and carbon dioxide were switched in the two bulbs, i.e. with driving forces of carbon dioxide and nitrogen in the same direction, no reverse diffusion of nitrogen would have been observed.

From the above discussions it should be clear that multicomponent mixtures exhibit transfer characteristics that are quite different from binary mixtures and a proper treatment of bulk diffusion in such mixtures must proceed along more mechanistic lines. The Maxwell–Stefan diffusion equations are capable of explaining all the curious phenomena that have been observed. The coupled diffusion effects observed by Duncan and Toor (1962) are not only of academic interest; such effects can have profound effects on the design of separation columns; see Krishna and Taylor (1986) and Taylor and Krishna (1992).

## COMBINED BULK AND KNUDSEN DIFFUSION

For gaseous mixtures at operating conditions under which the mean free path of the molecule is much larger than the pore diameter, molecule–wall collisions become more predominant than molecule–molecule collisions; the latter mechanism of transport is called the Knudsen diffusion. In the other limit when the mean free path of the molecule is much smaller than the pore diameter, molecule–molecule collisions predominate and bulk diffusion controls the diffusional transport. For the general case we need to take both molecule–wall and molecule–molecule collisions into account. Bulk and Knudsen diffusion processes occur in series (Fig. 10). The equations describing bulk diffusion have already been considered above. How do we combine the two distinct phenomena in a consistent manner? It is now generally agreed that the most convenient approach is to use the dusty gas model [see Jackson (1977), Mason and Malinauskas (1983) and Wesselingh and Krishna

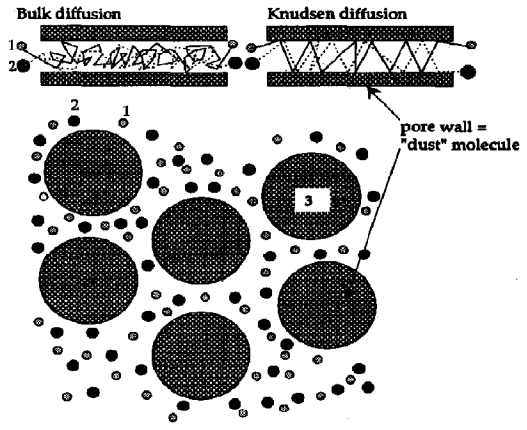


Fig. 10. Schematic picture of the dusty gas model in which the pore wall is modelled as giant dust molecules held motionless in space.

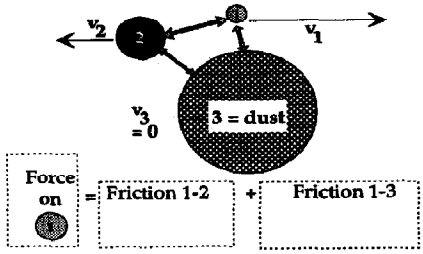


Fig. 11. The derivation of the dusty gas model. Note the similarity with the derivation of the Maxwell–Stefan diffusion equations for a ternary mixture (Fig. 9).

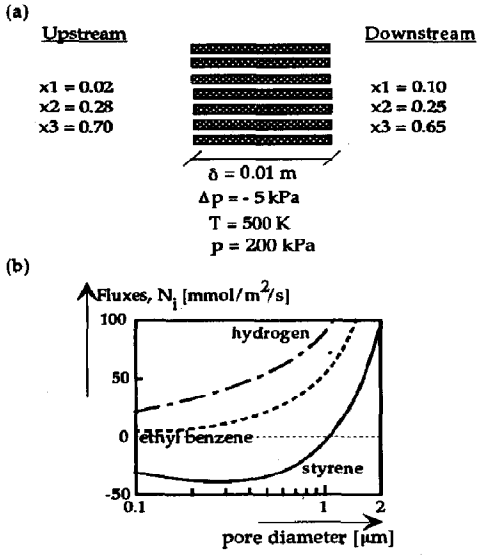


Fig. 12. Transport of the mixture styrene (1)–ethyl benzene (2)–hydrogen (3) across a porous membrane consisting of parallel capillaries. (a) The compositions at either end of the membrane, along with the temperature, pressure and membrane thickness. (b) Calculations of the fluxes of styrene, ethyl benzene and hydrogen as a function of the diameter of the capillaries.

(1990)]. The principle behind the dusty gas model is quite simple indeed and is really a straightforward application of the Maxwell–Stefan diffusion equations developed earlier. What we do is to consider the pore wall ("medium") as consisting of giant molecules ("dust") uniformly distributed in space. These dust molecules are considered to be a dummy, or pseudo, species $n+1$ in the $n$-component gaseous mixture (see Fig. 10). To develop the transport relations, we rely on our trustworthy Maxwell–Stefan diffusion equations (see Fig. 11). The force exerted on any species $i$ in the multicomponent mixture is balanced by friction between two molecular species $i$ and $j$ (i.e. bulk diffusion) together with the friction between the molecular species $i$ and the dummy species $n+1$ (dust):

$$-\nabla\mu_i = RT\sum_{j=1}^{n} x_j\frac{(\mathbf{v}_i-\mathbf{v}_j)}{\mathcal{D}_{ij}} + RTx_{n+1}\frac{(\mathbf{v}_i-\mathbf{v}_{n+1})}{\mathcal{D}_{i,n+1}} \qquad i=1,2,\ldots,n. \quad (24)$$

We may define the Knudsen diffusivity reflecting the molecule–wall (= dust) collision process as $\mathcal{D}_{i,Kn} = \mathcal{D}_{i,n+1}/x_{n+1}$; this diffusivity can be estimated from the kinetic gas theory. For a cylindrical pore of diameter $d_0$ the Knudsen diffusivity is $\mathcal{D}_{i,Kn} = (d_0/3)\sqrt{8RT/\pi M_i}$ where $M_i$ is the molar mass of species $i$. The dust molecules are held stationary in space and, therefore, $\mathbf{v}_{n+1}=0$. Equation (24) may be rewritten in terms of the fluxes $\mathbf{N}_i$ and we obtain the following extension of eq. (18a):

$$-\frac{1}{RT}\nabla p_i = \sum_{\substack{j=1\\ j\neq i}}^{n}\frac{x_j\mathbf{N}_i - x_i\mathbf{N}_j}{\mathcal{D}_{ij}} + \frac{\mathbf{N}_i}{\mathcal{D}_{i,Kn}} \qquad i=1,2,\ldots,n. \quad (25)$$

In order to get a feel for the dusty gas model for combined bulk and Knudsen diffusion, let us consider an example of diffusion in the gaseous mixture styrene (1)–ethyl benzene (2)–hydrogen (3) through an inert porous membrane made up of a bundle of parallel capillaries. Each capillary may be assumed to be cylindrical. The diagram of the membrane is shown in Fig. 12(a) along with the operating conditions. For steady-state diffusion across the membrane the fluxes $\mathbf{N}_i$ can be calculated by integrating the dusty gas model [eq. (25)]; details of the calculation procedure can be found in the worked example no. 25 of Wesselingh and Krishna (1990). These calculations have been carried out for various choices of the capillary pore diameter and the results are presented in Figure 12(b). The behaviour of ethyl benzene and hydrogen is as is to be expected; increase of the pore diameter increases the fluxes in a monotonic manner. The behaviour of styrene (1) is, on the other hand, quite remarkable. For pore diameters smaller than

0.4 $\mu$m, the styrene flux increases in magnitude as the pore diameter increases. For pore sizes in the range 0.4–2 $\mu$m the magnitude of styrene *decreases* with increasing pore size. For pore sizes larger than 2 $\mu$m the styrene flux changes direction and behaves "normally". The explanation of the curious behaviour of styrene is quite simple. For small pore diameters, towards the left side of the $x$-axis of Fig. 12(b), transport is in the Knudsen regime. In the Knudsen regime the relation between the flux and the driving force is [cf. eq. (25)]: $\mathbf{N}_i = -(\mathcal{D}_{i,Kn}/RT)\nabla p_i$; each of the three species diffuses independent of the others. As the pore diameter is increased, there is increased bulk diffusion contribution. In the bulk diffusion regime each species experiences a frictional drag with each of the other diffusing species. As already demonstrated by the Duncan and Toor example it is possible for a species tc be literally dragged up its composition gradient due to frictional drag with a heavy species moving in the opposite direction. For pore sizes greater than 2 $\mu$m, the bulk diffusion contribution is substantial enough for styrene to be transported against its composition gradient driving force.

In the literature on intraparticle diffusion within catalyst pellets it is common to use the Fick formulation, eq. (5), to describe intraparticle diffusion for combined bulk and Knudsen diffusion with the effective Fick diffusivity defined by

$$\frac{1}{D_{\text{eff}}} = \frac{1}{\mathcal{D}_{\text{bulk}}} + \frac{1}{\mathcal{D}_{Kn}}.$$

It can be verified from eq. (25) that this simplification is valid only in the limiting case when the bulk diffusivities of all the binary pairs are equal to one another $D_{ij} = D$ and if we have equimolar transfer $\mathbf{N}_t = \mathbf{0}$. For all other cases use of the simple Fick formulation can lead to difficulties; it would be impossible, for example, to model the behaviour of styrene in Fig. 12(b).

The numerical calculations in Figs 12(a) and (b) were carried out for cylindrical pores. For the general case of porous catalysts and adsorbents, each of diffusivities, bulk and Knudsen, will have to be corrected for the medium properties. This correction factor

$$(= \textit{porosity} \times \textit{constriction factor}/\textit{tortuosity})$$

can be determined from appropriate experiments.

A further complication which needs to be taken into account for diffusion in porous media is that the pressure gradient within catalysts and adsorbents is rarely negligible. Finite pressure gradients within catalysts and adsorbents engender an additional viscous flow contribution to the fluxes. The mixture velocity due to viscous flow is

$$\mathbf{v}_{\text{viscous}} = -\frac{B_0}{\eta}\nabla p \qquad (26)$$

where $B_0$ is the medium permeability, $\eta$ is the mixture viscosity and $\nabla p$ is the pressure gradient. For a cylindrical pore $B_0 = d_0^2/32$.

An interesting phenomenon occurs for intraparticle diffusion with heterogeneous chemical reaction within catalyst pellets. The flux ratio $\mathbf{N}_i/\mathbf{N}_j$ of components $i$ and $j$ participating in the reaction is dictated by the reaction stoichiometry. When the total mixture flux is non-zero (net production or consumption due to chemical reaction) there will be a finite pressure gradient developed inside the catalyst particle. This is illustrated in Fig. 13 for cracking and polymerisation-type reactions. Sometimes the pressure build-up as a consequence of reaction stoichiometry is large enough to cause concerns on mechanical strengths of the catalyst. Jackson (1977) has given a detailed discussion on influence of reaction stoichiometry on the developed pressure gradient. To give an illustration, if the reaction is a simple irreversible one involving two species A and B, A $\rightarrow m$B, where $m$ is the stoichiometric coefficient, the pressure at the centre of the catalyst pellet, assuming complete conversion of A, is $p_0 = \sqrt{mp}$, where $p$ is the pressure on the outside of the catalyst. Thus for $m = 2$, we have a 40% increase in pressure as we proceed towards the centre of the pellet (Jackson, 1977).

In the discussions above we have questioned the wisdom of using the Fick formulation for intraparticle bulk and Knudsen diffusion using the effective diffusivity

$$\frac{1}{D_{\text{eff}}} = \frac{1}{\mathcal{D}_{\text{bulk}}} + \frac{1}{\mathcal{D}_{Kn}}.$$

For any particular component in the multicomponent mixture we may, of course, force fit eq. (25) into the Fick form [eq. (5)] to obtain an expression for the effective diffusivity of that particular component. The effective diffusivity thus defined will be a strong function of the composition and also the flux ratios of all the species participating in say a chemical reaction within the pellet. Schnitzlein and Hofmann (1988) have presented calculations for the effective diffusivity for hydrogen in a gaseous mixture undergoing catalytic reforming (see Fig. 14). Use of the dusty gas model and the classic Wilke formula leads to significantly different effective diffusivity values for hydrogen. We also note that neglect of the viscous flow contribution is not very serious; this result is rather typical.

For multicomponent mixtures containing components of widely varying molar masses it is usually not justified to assume that either bulk or Knudsen diffusion "controls" the diffusional transport because of coupling between species diffusions. The use of the dusty gas model routinely is suggested for all calculations, especially for intraparticle diffusion with chemical reaction with selectivity considerations.

## SURFACE DIFFUSION OF ADSORBED MOLECULAR SPECIES

Let us now turn our attention to diffusion of adsorbed molecular species on the surface of an adsorbent or catalyst pellet. In developing our formulation for surface diffusion it is convenient to have

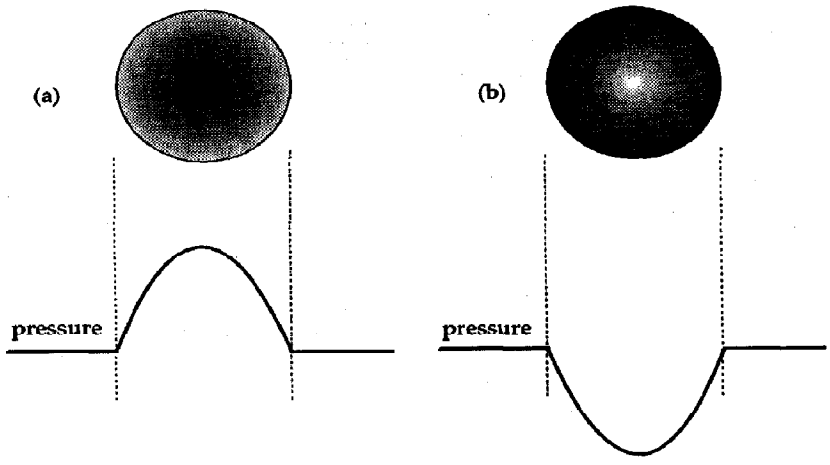


Fig. 13. Pressure profiles within porous catalyst particle for (a) cracking, and (b) "polymerization"-type reactions.

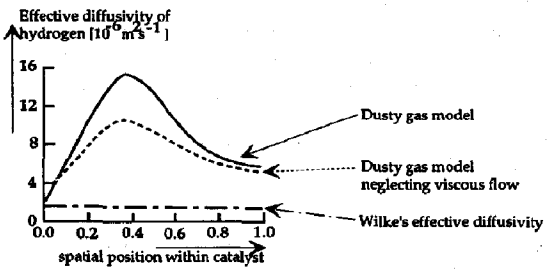


Fig. 14. Dependence of the effective diffusivity of hydrogen on the spatial position inside the catalyst particle for catalytic reforming of $C_7$ hydrocarbons (after Schnitzlein and Hofmann, 1988).

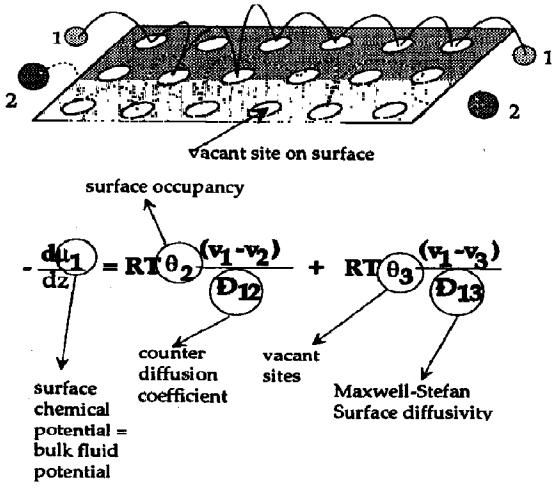


Fig. 15. The physical picture behind the Maxwell–Stefan formulation for surface diffusion. The vacant sites are pictured as pseudo-species in the treatment.

a simple physical picture for surface diffusion in mind. A simple physical model is depicted in Fig. 15 that shows molecules hopping from one adsorption site to another. A description of the hopping model can be found in Gilliland *et al.* (1974). If the adsorption sites are considered to be pseudo-species in the mixture, we may use the Maxwell–Stefan formulation to write the following expression for the driving force acting on the adsorbed species 1:

$$-\nabla\mu_i = RT\sum_{j=1}^{n}\theta_j\frac{(\mathbf{v}_i-\mathbf{v}_j)}{\mathcal{D}_{ij}^s} + RT\theta_{\mathrm{Vac}}\frac{(\mathbf{v}_i-\mathbf{v}_{\mathrm{Vac}})}{\mathcal{D}_{i,\mathrm{Vac}}^s} \qquad i=1,2,\ldots,n. \quad (27)$$

Here the $\mathcal{D}_{ij}^s$ and $\mathcal{D}_{i,\mathrm{Vac}}^s$ are the Maxwell–Stefan surface diffusivities. The coefficients $\mathcal{D}_{i,\mathrm{Vac}}^s$ are the single-component surface diffusivities and represent the facility of exchange between the sorbed species and the vacant sites, denoted by the subscript Vac. The Maxwell–Stefan formulation also allows the exchange between adsorbed species $i$ and $j$ at any adsorption site; thus, a site occupied by $i$ may be replaced by species $j$ or *vice versa*. The facility for counter-sorption is reflected by the coefficient $\mathcal{D}_{ij}^s$. The $\theta$s in eq. (27) represent the fractional occupancies of the adsorbed species. Thus, $\theta_i$ represents the fractional occupancy of the sites by the adsorbed species $i$ and $\theta_{\mathrm{Vac}}$ represent the fraction of unoccupied, vacant, sites $\theta_{\mathrm{Vac}} = 1-\theta_1-\theta_2-\cdots-\theta_n$. The surface chemical potential $\mu_i$ of species $i$ is given by the equilibrium relationship:

$$\mu_i = \mu_i^0 + RT\ln f_i \quad (28)$$

where $\mu_i^0$ is the surface chemical potential of adsorbed species at the chosen standard state and $f_i$ is the fugacity of species $i$ in the bulk fluid mixture (we

assume equilibrium between the bulk fluid and the surface in this discussion of surface diffusion alone).

The surface fluxes, $\mathbf{N}_i^s$, of the diffusing adsorbed species are defined as

$$\mathbf{N}_i^s = c^s \theta_i \mathbf{v}_i \tag{29}$$

where $c^s$ is the total saturation concentration on the surface. With this definition the Maxwell–Stefan surface diffusion [eq. (27)] may be recast in terms of the surface fluxes into the form analogous to eq. (18):

$$-\frac{\theta_i}{RT}\nabla\mu_i = \sum_{\substack{j=1 \\ j\neq i}}^{n} \frac{\theta_j \mathbf{N}_i^s - \theta_i \mathbf{N}_j^s}{c^s \mathcal{D}_{i,\mathrm{Vac}}^s} + \frac{\theta_{\mathrm{Vac}} \mathbf{N}_i^s - \theta_i \mathbf{N}_{\mathrm{Vac}}^s}{c^s \mathcal{D}_{i,\mathrm{Vac}}^s}$$

$$i = 1, 2, \ldots, n. \tag{30}$$

The surface chemical potential gradients may be expressed in terms of the gradients of the surface occupancies by introduction of the matrix of thermodynamics factors:

$$\frac{\theta_i}{RT}\nabla\mu_i = \sum_{j=1}^{n} \Gamma_{ij}\nabla\theta_j, \quad \Gamma_{ij} \equiv \theta_i \frac{\partial \ln f_i}{\partial \theta_j}$$

$$i, j = 1, 2, \ldots, n. \tag{31}$$

For the Langmuir isotherm, for example, the elements of $[\Gamma]$ are:

$$\Gamma_{ij} = \delta_{ij} + \frac{\theta_i}{\theta_{\mathrm{Vac}}}, \quad i, j = 1, 2, \ldots, n \tag{32}$$

Krishna (1990) has argued that one consequence of according the status of a pseudo-species to the adsorption sites (subscrpt Vac) is that the vacancy flux $\mathbf{N}_{\mathrm{Vac}}^s$ must balance the fluxes of the diffusing species $1, 2, \ldots, n$. In other words, for surface diffusion we always have equimolar diffusion, i.e. $\mathbf{N}_1^s + \mathbf{N}_2^s + \cdots + \mathbf{N}_{\mathrm{Vac}}^s = \mathbf{0}$. Other authors have not explicitly addressed the question of the status of the vacancy flux. We shall take up this point once again for discussions later in the paper.

*Surface diffusion of single component*

For the limiting case of single-component sorption eqs (30–(32) simplify to yield, in a manner analogous to eqs (12)–(14),

$$\mathbf{J}_1^s \equiv \mathbf{N}_1^s - \theta_1(\mathbf{N}_1^s + \mathbf{N}_{\mathrm{Vac}}^s) = -c^s \mathcal{D}_{1,\mathrm{Vac}}^s \Gamma \nabla\theta_1. \tag{33}$$

It is common in the literature on surface diffusion [see Ruthven (1984) and Yang (1987)] to define a Fick surface diffusivity

$$D_{1,\mathrm{Vac}}^s \equiv \frac{\mathbf{J}_1^s}{-c^s \nabla\theta_1} = \mathcal{D}_{1,\mathrm{Vac}}^s \Gamma. \tag{34}$$

The thermodynamic factor $\Gamma = 1/(1-\theta_1)$ for Langmuir adsorption and this factor shows a strong dependence on the surface coverage (see Fig. 16).

Mechanistically, the Maxwell–Stefan surface diffusivity may be related to the displacement of the adsorbed molecular species, $\lambda$, and the jump frequency, $\nu_1(\theta_1)$, which in general can be expected to be

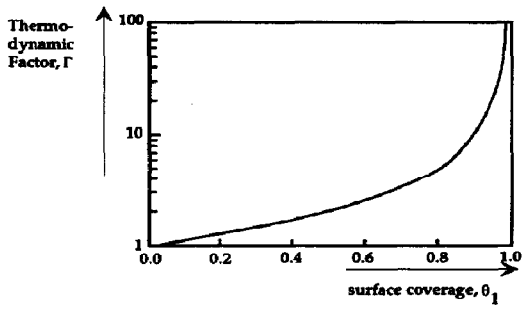


Fig. 16. The thermodynamic factor $\Gamma$ for single-component sorption, calculated for the Langmuir adsorption isotherm.

dependent on the surface coverage (Reed and Ehrlich, 1981; Zhdanov, 1985):

$$\mathcal{D}_{1,\mathrm{Vac}}^s = \lambda^2 \nu_1(\theta_1). \tag{35}$$

If the jump frequency $\nu_1(\theta_1) = \nu_1(0)$ remains constant, independent of surface coverage, the Maxwell–Stefan surface diffusivity $\mathcal{D}_{1,\mathrm{Vac}}^s$ is also independent of surface coverage. The Fick surface diffusivity in this case shows a strong increase with increased surface coverage. Figure 17, by way of illustration, shows the strong increase of the Fick surface diffusivity with surface coverage as experimentally observed by Pope (1967).

Another possibility is that due to interactions between adsorbed species the jump frequency decreases with surface coverage. If we assume that a molecule can migrate from one site to another only when the receiving site is vacant (see Barrer, 1978), the chance of this happening is proportional to $(1-\theta_1)$ so that

$$\nu_1(\theta_1) = \nu_1(0)(1-\theta_1)$$

$$\mathcal{D}_{1,\mathrm{Vac}}^s = \mathcal{D}_{1,\mathrm{Vac}(\theta_1\to 0)}^s (1-\theta_1). \tag{36}$$

For the behaviour of the Maxwell–Stefan surface diffusivity given by eq. (36), use of the Langmuir isotherm for calculation of the thermodynamic factor shows that the Fick surface diffusivity must remain constant and independent of surface coverage:

$$\mathcal{D}_{1,\mathrm{Vac}}^s = \mathcal{D}_{1,\mathrm{Vac}(\theta_1\to 0)}^s = \lambda^2 \nu_1(0). \tag{37}$$

Krishna (1990) assumed a Vignes-type relationship (16) to describe the decrease of the Maxwell–Stefan diffusivity with surface coverage:

$$\mathcal{D}_{1,\mathrm{Vac}}^s = (\mathcal{D}_{1,\mathrm{Vac}(\theta_1\to 1)}^s)^{\theta_1} (\mathcal{D}_{1,\mathrm{Vac}(\theta_1\to 0)}^s)^{1-\theta_1}. \tag{38}$$

*Tracer diffusion*

In tracer diffusion experiments we consider exchange between

$$\mathbf{J}_1^s = -\mathbf{J}_2^s, \quad \nabla\theta_1 = -\nabla\theta_2. \tag{39}$$

We may apply the Maxwell–Stefan equations (30) and (31) with the above simplifications (39) to obtain the following explicit expression for the tracer diffusivity

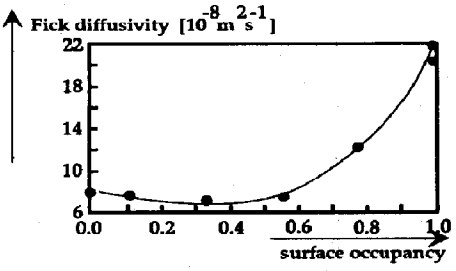


Fig. 17. Fick surface diffusivity as function of surface coverage for the system sulphur dioxide–microporous spheron 6 (data from Pope, 1967).

[see Krishna (1990) for detailed derivation].

$$\mathbf{J}_1^s = -c^s D_1^* \nabla\theta_1, \quad \frac{1}{D_1^*} = \frac{\theta_1 + \theta_2}{Đ_{12}^s} + \frac{\theta_{Vac}}{Đ_{1,Vac}^s}. \tag{40}$$

If the counter-exchange coefficient $Đ_{12}^s = Đ_{1,Vac}^s = Đ_{2,Vac}^s$ then we have the equality between the tracer diffusivity and the Maxwell–Stefan surface diffusivity:

$$D_1^* = Đ_{1,Vac}^s \tag{41}$$

which equality has been verified experimentally (cf. Goddard and Ruthven, 1986). When the Maxwell–Stefan surface diffusivity is surface coverage independent (i.e. constant jump frequency), the tracer diffusivity is also independent of surface coverage. When the Maxwell–Stefan surface diffusivity is proportional to $(1 - \theta_1)$, i.e. follows the relationship (36), the tracer diffusivity also shows this dependence; this is the model of Riekert (1971).

*Binary sorption kinetics*

For uptake of two components we need to reckon with the complete set of Maxwell–Stefan diffusion equations; Krishna (1990) has worked out the details of this procedure using matrix algebra and obtained explicit expressions for the Fick matrix of surface diffusivities defined by

$$(\mathbf{J}^s) = -c^s[D^s](\nabla\theta) = -c^s[B^s]^{-1}[\Gamma](\nabla\theta) \tag{42}$$

where the surface diffusion fluxes $\mathbf{J}_i^s$ are defined, as in the rest of the paper, with respect to the molar average mixture velocity $\mathbf{v}$; cf. eq. (4). The value of the Fick diffusivity depends on the choice of reference velocity frame. The explicit expression for the matrix $[B^s]$ is consequently also dependent on the choice of the reference velocity frame. For the molar average reference velocity frame the elements of $[B^s]$ for binary sorption are given by eq. (22) using the surface coverages $\theta_i$ in place of the mole fractions $x_i$ and the Maxwell–Surface diffusivities $Đ_{ij}^s$ in place of the $Đ_{ij}$.

In case of diffusion inside the pores of a zeolite there is no possibility of two different molecules undergoing counter-exchange at an adsorption site. In other words, the "drag" contributions, reflected by the first right members of eqs (27) and eq. (30), are not present. In the literature on binary sorption kinetics within zeolites it is common to assume such a "single-file diffusion" mechanism. On close examination of the literature on this subject [e.g. Qureshi and Wei (1990)], it appears that most authors define the matrix of Fick surface diffusivities not in the molar average reference frame (as for single-component sorption) but in a reference velocity frame relative to the vacant sites ("solvent" fixed reference frame in the terminology of the literature on bulk fluid diffusion). The expression for the Fick surface diffusivity matrix used by Qureshi and Wei (1990) [cf. their eq. (6)] is

$$[D^s] = \lambda^2 \begin{bmatrix} \nu_1(0) & 0 \\ 0 & \nu_2(0) \end{bmatrix} \begin{bmatrix} 1-\theta_2 & \theta_1 \\ \theta_2 & 1-\theta_1 \end{bmatrix} \tag{43}$$

along with the equation of continuity in the form [cf. their eq. (5)]

$$\frac{\partial(\theta)}{\partial t} = \nabla\cdot[[D^s]\nabla(\theta)]. \tag{44}$$

It is an interesting and instructive exercise to try to derive the relations (43) and (44) used by Qureshi and Wei using our general approach; in this manner we make transparent all the tacit assumptions made by these authors. The first point concerns the choice of the reference velocity frame for surface diffusion. Use of eqs (43) and (44) implies the use of a reference velocity frame with respect to the vacant sites. Further, Qureshi and Wei assume a vanishing vacancy flux $N_{Vac}^s = 0$. With these assumptions we obtain from eqs (30) and (31)

$$\mathbf{N}_i^s = -c^s \frac{Đ_{i,Vac}^s}{\theta_{Vac}} \sum_{j=1}^{n} \Gamma_{ij}\nabla\theta_j, \quad i = 1, 2, \ldots, n. \tag{45}$$

If the Maxwell–Stefan surface diffusivities, $Đ_{i,Vac}^s$, decrease with the surface occupancy, following the relations (35) and (36) we get

$$Đ_{i,Vac}^s = Đ_{i,Vac(\theta_i\to 0)}^s(1-\theta_t) = \lambda^2\nu_i(0)(1-\theta_t) \tag{46}$$

where $\theta_t = 1 - \theta_{Vac}$ is the total occupancy of the species 1, 2, . . . , $n$. The explicit expression for the matrix of Fick surface diffusivities follows from eqs (42), (45) and (46):

$$[D^s] = \lambda^2 \begin{bmatrix} \nu_1(0) & 0 \\ 0 & \nu_2(0) \end{bmatrix} \frac{\begin{bmatrix} 1-\theta_2 & \theta_1 \\ \theta_2 & 1-\theta_1 \end{bmatrix}}{1-\theta_1-\theta_2} \tag{47}$$

where the second term on the right-hand side of eq. (47) is the thermodynamic factor. A close examination of eqs (43)–(47) shows that in order to derive the expression of Qureshi and Wei (1990), eq. (43), we need to adopt the model $\nu_i = \nu_i(0)(1-\theta_t)^2$, i.e. $Đ_{i,Vac}^s = Đ_{i,Vac(\theta_t\to 0)}^s(1-\theta_t)^2$.

In order to compare the result (47) with the model used by Habgood (1958) and Round *et al.* (1966), we

*define* effective surface diffusivities for each of the components 1 and 2 in the binary mixture by the relations

$$\frac{\partial \theta_i}{\partial t} = \nabla \cdot (D^s_{i,\text{eff}} \nabla \theta_i), \quad i = 1, 2. \tag{48}$$

On comparison with eqs (44) and (47), we obtain the following expressions for the effective diffusivities:

$$D^s_{1,\text{eff}} = \frac{\mathcal{D}^s_{1,\text{Vac}(\theta_i \to 0)}}{1 - \theta_1 - \theta_2}\left((1 - \theta_2) + \theta_1 \frac{\nabla \theta_2}{\nabla \theta_1}\right) \tag{49}$$

and

$$D^s_{2,\text{eff}} = \frac{\mathcal{D}^s_{2,\text{Vac}(\theta_i \to 0)}}{1 - \theta_1 - \theta_2}\left((1 - \theta_1) + \theta_2 \frac{\nabla \theta_1}{\nabla \theta_2}\right). \tag{50}$$

The above expressions for the effective surface diffusivities in a binary mixture coincide precisely with those given by Habgood (1958) and Round *et al.* (1966). It is clear from eqs (49) and (50) that the effective surface diffusivities are strong functions of surface concentrations and surface concentration *gradients*. Farooq and Ruthven (1991) have used the expressions (49) and (50) to simulate, with considerable success, a kinetically controlled pressure swing adsorption process.

It is important not to lose track of the major benefit of the Maxwell–Stefan formulations for surface diffusion: we are able to predict binary sorption kinetics on the basis of information on single-component sorption, along with multicomponent equilibrium thermodynamics (i.e. the adsorption isotherm). This should be clear from the expression (47). The first member on the right-hand side can be obtained from single-component sorption kinetics. The second member on the right-hand side reflects multicomponent adsorption equilibria. The element of the Fick surface diffusivity matrix $[D^s]$ portrays a conglomerate of these two effects namely: (i) the surface mobility of the adsorbed species 1 and 2, and (ii) the fluid–solid adsorption equilibrium ("isotherm"). This matrix is almost always non-diagonal with large off-diagonal elements. In order to illustrate the consequence of a non-diagonal matrix $[D^s]$, let us consider the example of the uptake of a mixture of benzene (1) and *n*-heptane (2) by NaX zeolite. The zeolite crystals are exposed to a bulk vapour mixture maintaining a constant composition environment of benzene and *n*-heptane and the uptake of these components by the zeolite is monitored as a function of time. The observed transient uptake profiles as measured experimentally by Kärger and Bülow (1975) are shown in Fig. 18(a). The profile for *n*-heptane (2) exhibits a remarkable maximum at $t = 50$ min in the uptake profile, with the surface concentration reaching a value significantly higher than the final (low) equilibrium surface concentration value. The results can be explained physically as follows. The surface mobility, reflected in the Maxwell–Stefan surface diffusivity, of *n*-heptane $\mathcal{D}^s_{2,\text{Vac}(\theta_i \to 0)}$ is about 50 times larger than the corresponding mobility of benzene, $\mathcal{D}^s_{1,\text{Vac}(\theta_i \to 0)}$, due to molecular configurational considerations. Initially, therefore, *n*-heptane quickly penetrates the pores of the zeolite occupying the adsorption sites. The adsorption strength of *n*-heptane is, however, considerably lower than that of benzene due *inter alia* to differences in polarity. Beyond $t = 50$ min, the adsorbed *n*-heptane gets (slowly) displaced from the active sites by benzene and the surface concentration of *n*-heptane decreases from its maximum value to reach, eventually, its final low equilibrium concentration. At equilibrium, achieved after about 5 h, the pores of the zeolite are occupied predominantly by the strongly adsorbed benzene. From the point of view of developing a separation process to separate benzene from *n*-heptane it appears that two type of processes are possible. The first one is based on equilibrium selectivity requiring about 5 h; here the zeolite pores contain predominantly benzene. The other alternative is to use diffusion selectivity and terminate the uptake process at $t = 50$ min; here the pores of the zeolite contain *n*-heptane to a predominant extent. Diffusion selectivity requires significantly shorter residence times and may offer some technological advantages.

The transient uptake process can be simulated by solving the equations of continuity, eq. (1), together with the constitutive equation for binary sorption: eqs (42). Simulations using eq. (47) for the Fick surface diffusivity matrix are shown in Fig. 18(b); it is clear that the constitutive equations (42), (46) and (47) are able to reflect all the features of the measured profiles. The use of uncoupled surface diffusion equations would lead to monotonic equilibration of both species [cf. Krishna (1990)] confirming the need to properly separate kinetic "drag" and thermodynamic factors.

In an attempt to verify the applicability of the Maxwell–Stefan diffusion equations for diffusion inside zeolites, van den Broeke *et al.* (1992) have resorted to Monte Carlo simulations. A sample of their simulation results for binary uptake of benzene and *n*-heptane is shown in Fig. 19(a), which is comparable with the Maxwell–Stefan simulations presented in Fig. 18(b).

It is proper to point out here that Round *et al.* (1966) were probably the first to present a detailed analysis of diffusion of binary sorbed species. Their treatment is essentially equivalent to the one presented here.

*Ternary sorption kinetics*

The set of eqs (30) and (31) is valid for *n*-component surface diffusion. The constitutive equations for single diffusion are given by eqs (45) and (46) and the solution of the constitutive equations (1) yields the description of ternary sorption kinetics. In an attempt to verify the applicability of the Maxwell–Stefan surface (micropore) diffusion formulation for multicomponent mixtures, van den Broeke *et al.* (1992) have also carried out Monte Carlo simulations for uptake of a ternary mixture within a zeolite pore; a sample of their results is shown in Fig. 19(b). We see that a ternary mixture exhibits two maxima. It should, therefore,

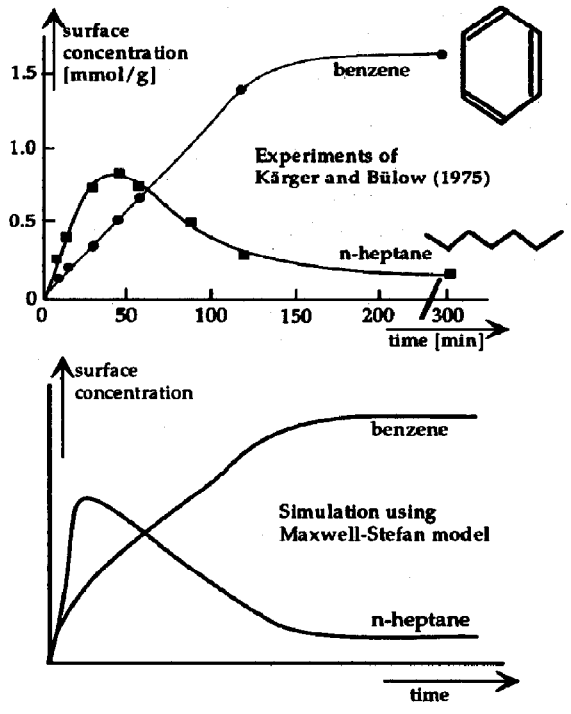


Fig. 18. Transient uptake of benzene and *n*-heptane by zeolite X. Comparison of (a) experimental results of Kärger and Bülow (1975) with (b) simulations using the Maxwell–Stefan surface diffusion model.

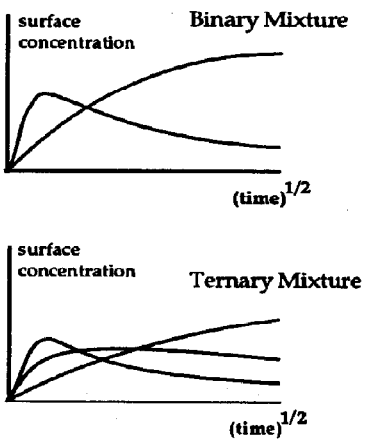


Fig. 19. Monte Carlo simulations for transient uptake of binary and ternary mixtures within pores of a zeolite. The simulations were carried out using the single-file diffusion model (after van den Broeke *et al.*, 1992).

be possible, in principle, to develop a separation process for separating the three components by relying on diffusion selectivity and "tapping" off at time intervals corresponding to the respective maxima. A good appreciation of the fundamental mechanisms of surface (micropore) diffusion will, we believe, lead to the development of new separation processes based on diffusion selectivity.

## COMBINED BULK, KNUDSEN AND SURFACE DIFFUSION

Within the pores of a sorbent we have, in general, a combination of the three diffusion mechanisms, pictured in Fig. 3, along with the additional non-separative contribution of viscous flow. The total flux of any species is obtained by combining the separate contributions; it is helpful in this regard to keep the electric analogue circuit in mind (see Fig. 20). For diffusion inside macropores all contributions may be important. In order to demonstrate this, we present the experimental results of Sloot (1991) on the total flux of $H_2S$ through a catalytic membrane made up of $\alpha$-alumina with a mean pore diameter of 350 nm, impregnated with $\gamma$-alumina, the catalyst for the Claus reaction (see Fig. 21). The experimental results of Sloot (1991) show that, despite the relatively large pore size, there is a very significant contribution due to surface diffusion, amounting to about 60–80% of bulk and Knudsen contributions. The high surface diffusion contribution is to be attributed to the strong adsorption of $H_2S$.

Setting up of the Maxwell–Stefan diffusion equations for combined bulk, Knudsen and surface diffusion is a straightforward combination of the formalisms developed earlier in this paper. It is helpful to

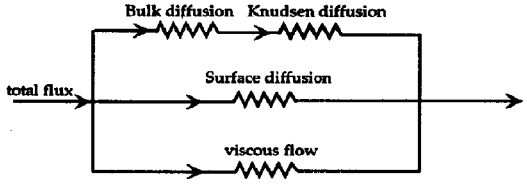


Fig. 20. Electric analogue circuit picturing the flux of the diffusing species within a porous medium (after Mason and Malinauskas, 1983).

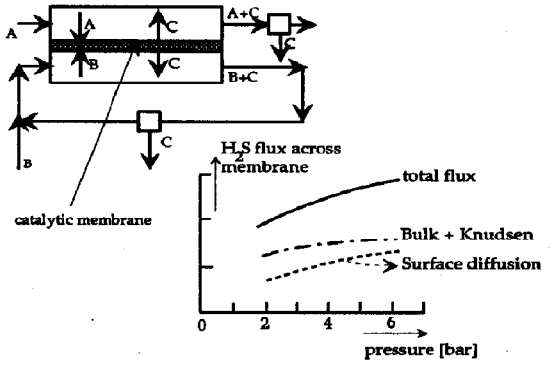


Fig. 21. Contributions of bulk, Knudsen and surface diffusion for transfer of $H_2S$ across a catalytic membrane carrying the Claus reaction: $2H_2S + SO_2 \rightleftharpoons \frac{3}{8}S_8 + 2H_2O$ (after Sloot, 1991).

have a physical picture of the combined phenomena in mind. Towards this end we propose the crated dusty gas model. The large dust molecules, of infinite molar mass, representing the medium have craters on its exterior surface representing the adsorption sites (see Fig. 22). Molecule–molecule collisions and molecule–dust collisions occurring in series, result, respectively, in bulk and Knudsen diffusion. In addition each of the molecular species may be adsorbed on the active sites of the medium. These vacant sites are also accorded the status of pseudo-species, of vanishing molar mass, and may be thought of as being akin to craters on a golf ball. The adsorbed species move ("hop" or "jump") from one crater to another and may undergo desorption to the bulk fluid phase.

Hu and Do (1992) present experimental results for transient uptake of ethane and *n*-butane on to activated carbon at 30°C and 101.35 kPa. Their experimental results are presented in Fig. 23, wherein it is to be noted that the fractional uptake of each of the species is normalised with its own final equilibrium concentration. It is for this reason that the fractional uptake of each species approaches unity at equilibrium. The uptake profile for ethane exhibits a maximum at $t = 40$ s; this maximum concentration is about three times larger than its equilibrium concentration. We note the striking similarity of the transient uptake profiles in Fig. 23 with the results presented in Fig. 18 for uptake of benzene and *n*-heptane in NaX zeolite. The smooth curves presented in Fig. 23 represent the simulations of Hu and Do (1992) using a combined model with bulk, Knudsen and surface diffusion. For the Fick surface diffusivity matrix Hu and Do (1992) use the relation

$$[D^s] = \begin{bmatrix} \mathcal{D}^s_{1,\mathrm{Vac}(\theta_t \to 0)} & 0 \\ 0 & \mathcal{D}^s_{2,\mathrm{Vac}(\theta_t \to 0)} \end{bmatrix} [\Gamma]. \quad (51)$$

For the calculation of the thermodynamic factor matrix $[\Gamma]$, Hu and Do (1992) make use of the relation (31). The simulations are able to reproduce the essential character of the experimentally observed profiles.

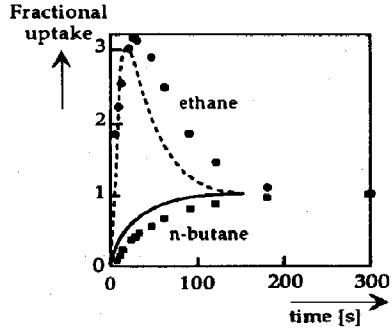


Fig. 23. Transient uptake of ethane and *n*-butane by activated carbon, in which both micropore and macropore resistances are significant (after Hu and Do, 1992).

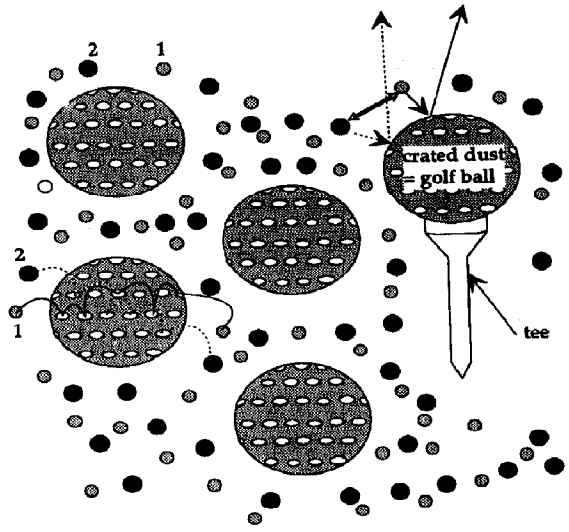


Fig. 22. The three mechanisms of bulk, Knudsen and surface diffusion can be integrated into a common physical picture in which the porous medium is modelled as giant dust molecules (golf balls), with craters representing the adsorption sites.

## CLOSING REMARKS

In this paper we have attempted to model intraparticle diffusion inside a porous medium in a unified consistent manner using a simple mechanistic picture of diffusion: To move a species with respect to other species (i.e. to allow a species to diffuse), we must exert a force on it; this force is the gradient of the chemical potential. During species diffusion, drag is encountered with other molecular species and we have a balance between the applied force and frictional drag with the other molecular species. Using this simple, hydrodynamic, model, i.e. the Maxwell–Stefan formulation, we set out to model, in turn, bulk, Knudsen and surface diffusion. Throughout the discussions we have tried to point out the shortcomings of the commonly used Fick formulation to describe each of the three diffusion mechanisms inside porous particles. The Fick formulation has been shown to fail even at the qualitative level to explain the observed diffusion phenomena such as osmotic diffusion, diffusion barrier and reverse diffusion.

The major advantage of the Maxwell–Stefan formulation is that it is possible, in principle, to predict the behaviour of a multicomponent mixture on the basis of the following information:

(i) Maxwell–Stefan binary pair diffusivities: $\mathcal{D}_{ij}$, $\mathcal{D}_{i,Kn}$ and $\mathcal{D}^s_{i,\mathrm{Vac}}$, which may be obtained from *binary* experimental data; and

(ii) *multicomponent* solution thermodynamics; in particular, the matrix of thermodynamic factor $[\Gamma]$ in the bulk fluid mixture [cf. eq. (20)] and on the surface [cf. eq. (31)].

For bulk and Knudsen diffusion of ideal gas mixtures in porous media, the theory (the dusty gas model) is almost fully developed but there are still a few unanswered questions in the development of the theory of multicomponent surface diffusion of adsorbed species, including those concerning the choice of the reference velocity frame. The crated dusty gas (golf ball) model has been suggested as a tenable physical picture to be used for combining all three diffusion mechanisms.

It has been suggested in the discussions that a proper understanding and modelling of the diffusion processes may provide new ideas for the development of diffusion-selective adsorption processes.

*Acknowledgement*—The author expresses his gratitude to the referee for drawing attention to the basis of the derivation of eq. (43).

## NOTATION

| | |
|---|---|
| $B_0$ | permeability, $m^2$ |
| $[B]$ | matrix of inverted Maxwell–Stefan diffusivities defined in eq. (22), $m^{-2} s^1$ |
| $c$ | molar concentration of the mixture, $mol\,m^{-3}$ |
| $c_i$ | molar concentration of species $i$, $mol\,m^{-3}$ |
| $c^s$ | total saturation concentration of surface, $mol\,m^{-2}$ |
| $d_0$ | pore diameter, m |
| $D$ | Fick diffusivity in binary mixture, $m^2\,s^{-1}$ |
| $[D]$ | matrix of Fick diffusivities for multicomponent system, $m^2\,s^{-1}$ |
| $Đ_{12}$ | Maxwell–Stefan diffusivity in bulk fluid phase, $m^2\,s^{-1}$ |
| $Đ_{i,Kn}$ | Knudsen diffusivity of component $i$, $m^2\,s^{-1}$ |
| $Đ^s_{ij}$ | counter-sorption Maxwell–Stefan diffusivity, $m^2\,s^{-1}$ |
| $Đ^s_{i,\mathrm{Vac}}$ | single-component surface diffusivity, $m^2\,s^{-1}$ |
| $D^*_1$ | tracer diffusivity of component 1, $m^2\,s^{-1}$ |
| $D^s_{1,\mathrm{eff}}$ | effective surface diffusivity, $m^2\,s^{-1}$ |
| $f_i$ | fugacity of species $i$; $f_i = p_i$ for ideal gases, Pa |
| $[I]$ | identity matrix with elements $\delta_{ij}$, dimensionless |
| $(J)$ | column vector of diffusion fluxes, $mol\,m^{-2}\,s^{-1}$ |
| $\mathbf{J}_i$ | diffusion flux of species $i$ relative to the molar average reference velocity, $\mathbf{v}$, $mol\,m^{-2}\,s^{-1}$ |
| $m$ | stoichiometric coefficient of reaction, dimensionless |
| $M_i$ | molar mass of species $i$, $kg\,mol^{-1}$ |
| $n$ | number of diffusing species, dimensionless |
| $\mathbf{N}_i$ | molar flux of species $i$ in a stationary coordinate frame of reference, $mol\,mol^{-2}\,s^{-1}$ |
| $\mathbf{N}^s_i$ | surface flux, $mol\,m^{-1}\,s^{-1}$ |
| $p$ | system pressure, Pa |
| $p_i$ | partial pressure of species $i$, Pa |
| $R$ | gas constant, 8.314 $J\,mol^{-1}\,K^{-1}$ |
| $\mathscr{R}_i$ | is the rate of production of $i$ due to chemical reaction within the pellet, $mol\,m^{-3}\,s^{-1}$ |
| $t$ | time, s |
| $T$ | absolute temperature, K |
| $\mathbf{v}_i$ | is the velocity of the diffusing species $i$, $m\,s^{-1}$ |
| $v_1, v_2$ | $z$-coordinate velocities of species 1 and 2, $m\,s^{-1}$ |
| $\mathbf{v}$ | molar average mixture velocity, $m\,s^{-1}$ $\left(= \sum_{i=1}^{n} x_i \mathbf{v}_i\right)$ |
| $x_i$ | mole fraction of species $i$ |
| $\nabla x_i$ | gradient of the component mole fraction can be regarded as the driving force for diffusion. |
| $z$ | direction coordinate, m |

*Greek letters*

| | |
|---|---|
| $\gamma_i$ | activity coefficient of species $i$ in mixture, dimensionless |
| $\Gamma$ | thermodynamic correction factor for binary mixture, dimensionless |
| $[\Gamma]$ | matrix of thermodynamic factors, dimensionless |
| $\delta_{ij}$ | Kronecker delta ($= 1$ if $i = j$; $= 0$ if $i \neq j$), dimensionless |
| $\theta_i$ | fractional surface occupancy of component $i$, dimensionless |
| $\lambda$ | lateral displacement during surface diffusion, m |
| $\eta$ | fluid mixture viscosity, Pa s |
| $\mu_i$ | molar chemical potential, $J\,mol^{-1}$ |
| $\nu_1$ | jump frequency of component 1, $s^{-1}$ |

*Subscripts*

| | |
|---|---|
| $i, j$ | components in mixture |
| eff | effective parameter |
| $Kn$ | Knudsen coefficient |
| $t$ | total mixture |
| viscous | viscous flow parameter |
| $x_1 \to 0$ | for vanishing small concentration of species 1 |
| $x_1 \to 1$ | for almost pure component 1 |

*Superscripts*

| | |
|---|---|
| $s$ | surface |
| 0 | standard state |

## REFERENCES

Barrer, R. M., 1978, *Zeolites and Clay Minerals as Sorbents and Molecular Sieves*. Academic Press, London.

Bird, R. B., Stewart, W. E. and Lightfoot, E. N., 1960, *Transport Phenomena*. Wiley, New York.

Clark and Rowley, 1986, The mutual diffusion coefficient of methanol–*n*-hexane near the consolute point. *A.I.Ch.E. J.* **32**, 1125–1131.

Duncan, J. B. and Toor, H. L., 1962, An experimental study of three component gas diffusion. *A.I.Ch.E. J.* **8**, 38–41.

Farooq, S. and Ruthven, D. M., 1991, Numerical simulation of a kinetically controlled pressure swing adsorption bulk separation process based on a diffusion model. *Chem. Engng Sci.* **46**, 2213–2224.

Goddard, M., and Ruthven, D. M., 1986, Sorption and diffusion of C aromatic hydrocarbons in faujasite-type zeolites III. Self-diffusivities by tracer exchange. *Zeolites* **6**, 445–448.

Gilliland, E. R., Baddour, R. F., Perkinson, G. P. and Sladek, K. J., 1974, Diffusion on surfaces. I. Effect of concentration on the diffusivity of physically adsorbed gases. *Ind. Engng Chem. Fundam.* **13**, 95–100.

Habgood, H. W., 1958, The kinetics of molecular sieve action. Sorption of nitrogen–methane mixtures by Linde molecular sieve 4A. *Can. J. Chem.* **36**, 1384–1397.

Hu, X. and Do, D. D., 1992, Multicomponent adsorption kinetics of hydrocarbons onto activated carbon: effect of adsorption equilibrium equations. *Chem. Engng Sci.* **47**, 1715–1725.

Jackson, R., 1977, *Transport in Porous Catalysts*. Elsevier, Amsterdam.

Kärger, J. and Bülow, M., 1975, Theoretical prediction of uptake behaviour in adsorption of binary gas mixtures using irreversible thermodynamics. *Chem. Engng Sci.* **30**, 893–896.

Krishna, R., 1990, Multicomponent surface diffusion of adsorbed species: a description based on the generalized Maxwell–Stefan equations. *Chem. Engng Sci.* **45**, 1779–1791.

Krishna, R., 1987, A unified theory of separation processes based on irreversible thermodynamics. *Chem. Engng Commun.* **59**, 33–64.

Krishna, R. and Taylor, R., 1986, Multicomponent mass transfer: theory and applications, in *Handbook for Heat and Mass Transfer Operations* (Edited by N. P. Cheremisinoff), Chapter 7, Vol. 2. Gulf Publishing Corporation, Houston.

Maxwell, J. C., 1867, On the dynamical theory of gases. *Phil. Trans. R. Soc.* **157**, 49.

Mason, E. A. and Malinauskas, A. P., 1983, *Gas Transport in Porous Media: the Dusty Gas Model*. Elsevier, Amsterdam.

Pope, C. G., 1967, Flow of sulphur dioxide over the surface of spheron 6(2700) graphitized carbon black. *Trans. Faraday Soc.* **63**, 734–742.

Qureshi, W. R. and Wei, J., 1990, One- and two-component diffusion in zeolite ZSM-5. I. Theoretical. *J. Catal.* **126**, 126–146.

Reed, D. A. and Ehrlich, G., 1981, Surface diffusion, atomic jump rates and thermodynamics. *Surface Sci.* **102**, 588–609; *Surface Sci.* **105**, 603–628.

Riekert, L., 1971, Rates of sorption and diffusion of hydrocarbons in zeolites. *A.I.Ch.E. J.* **17**, 446–454.

Round, G. F., Habgood, H. W. and Newton, R., 1966, A numerical analysis of surface diffusion in a binary adsorbed film. *Separat. Sci.* **1**, 219–244.

Ruthven, D. M., 1984, *Principles of Adsorption and Adsorption Processes*. Wiley, New York.

Schnitzlein, K. and Hofmann, H., 1988, Solving the pellet problem for multicomponent mass transport and complex reactions. *Comput. Chem. Engng* **12**, 1157–1161.

Sloot, H. J., 1991, A non-permslective membrane reactor for catalytic gas phase reactions. Ph.D. thesis in Chemical Engineering, University of Twente, Enschede.

Stefan, J., 1871, Über das Gleichgewicht und die Bewegung insbesondere die Diffusion von Gasgemengen. *Sitzber. Akad. Wiss. Wien* **63**, 63.

Taylor, R. and Krishna, R., 1992, *Multicomponent Mass Transfer*. Wiley, New York (to be published).

Toor, H. L., 1957, Diffusion in three component gas mixtures. *A.I.Ch.E. J.* **3**, 198–207.

van den Broeke, L. J. P., Nijhuis, S. and Krishna, R., 1992, Monte Carlo simulations of diffusion in zeolites and comparison with the generalised Maxwell–Stefan theory. *J. Catal.* (in press).

Vignes, A., 1966, Diffusion in binary solutions. *Ind. Engng Chem. Fundam.* **5**, 189–199.

Wesselingh, J. A. and Krishna, R., 1990, *Mass Transfer*. Ellis Horwood, Chichester.

Yang, R. T., 1987, *Gas Separation by Adsorption Processes*. Butterworth, Boston.

Zhdanov, V. P., 1985, General equations for description of surface diffusion in the framework of the lattice gas model. *Surface Sci.* **194**, L13–L17.